

Sample Complexity of Probabilistic Roadmaps via ϵ -nets

Matthew Tsao, Kiril Solovey, and Marco Pavone

Abstract—We study fundamental theoretical aspects of probabilistic roadmaps (PRM) in the finite time (non-asymptotic) regime. In particular, we investigate how completeness and optimality guarantees of the approach are influenced by the underlying deterministic sampling distribution \mathcal{X} and connection radius $r > 0$. We develop the notion of (δ, ϵ) -completeness of the parameters \mathcal{X}, r , which indicates that for every motion-planning problem of clearance at least $\delta > 0$, PRM using \mathcal{X}, r returns a solution no longer than $1 + \epsilon$ times the shortest δ -clear path. Leveraging the concept of ϵ -nets, we characterize in terms of lower and upper bounds the number of samples needed to guarantee (δ, ϵ) -completeness. This is in contrast with previous work which mostly considered the asymptotic regime in which the number of samples tends to infinity. In practice, we propose a sampling distribution inspired by ϵ -nets that achieves nearly the same coverage as grids while using significantly fewer samples.

I. INTRODUCTION

The Probabilistic Roadmap Method (PRM) [1] is one of the most popular and widely used sampling-based technique for motion planning. PRM strives to provide a graph approximation of the full free space of the problem, by generating a set of configuration samples and connecting nearby samples when it is possible to move between configurations without collision using straight-line paths. As such it is particularly suitable in multi-query settings, where the same workspace environment needs to be preprocessed in order to answer multiple queries consisting of different start and goal points. In this context, PRM has been applied to various challenging robotic settings in recent years, including manipulation planning [2], inspection planning and coverage [3], task planning [4], and multi-robot motion planning [5], [6]. PRM also plays an important role in many modern single-query planners, which maintain an implicitly represented PRM graph—a portion of which is constructed on the fly—and return a solution that minimizes the path’s cost [7], [8], [9], [10], [11].

Due to this prolific utility, extensive study of PRM’s theoretical properties quickly followed its inception. The main question that occupied the research community at first was whether PRM guarantees to find a solution if one exists [12], [13], [14], and later on the quality of the returned solution. With respect to the latter question, several works have established the magnitude of the connection radius r sufficient to guarantee the convergence of the solution returned by PRM to an optimal solution [15]. However, the majority of works addressing those two questions consider in their analysis the (somewhat unrealistic) asymptotic regime, in which it is assumed that the number of samples n tends to infinity. *And so, the question of what are the smallest values of n, r to guarantee a high-quality solution in practice, i.e., when n is fixed, remains open.*

Statement of Contributions: In this work we make progress toward addressing the aforementioned question. In particular, we study how the sample set \mathcal{X} , and its cardinality n , as well

as the size of the connection radius r , affect completeness and optimality guarantees of PRM. Central to our contribution is the notion of (δ, ϵ) -completeness of the parameters \mathcal{X}, r , which indicates that for every motion-planning problem of clearance at least $\delta > 0$, PRM using \mathcal{X}, r returns a solution no longer than $1 + \epsilon$ times the shortest path that has at least δ clearance from the obstacles.

The mathematical concept of ϵ -nets (see, e.g., [16]) plays a key role in our contributions in both the theory and application. From a theoretical perspective, we leverage properties of ϵ -nets to characterize in terms of lower and upper bounds the sample size and connection radius needed to guarantee (δ, ϵ) -completeness. This is in contrast with previous work which mostly considered the asymptotic regime in which the number of samples tends to infinity.

From an application perspective, we leverage properties of ϵ -nets to produce sample sets that efficiently cover the workspace. We observe empirically that these sample sets offer nearly the same dispersion as grids while using significantly fewer samples. Grids are an important baseline because they are used widely in practice and offer better coverage (i.e. dispersion) than uniform random sampling [17]. The increased efficiency provided by these sample sets which we propose here can improve the runtime of PRM and related algorithms.

This paper is organized as follows. A survey of related work is presented in Section II. We review foundational ideas and establish notation in Section III. Section IV presents the main theoretical contributions and Section V presents proof sketches for some of the results. Numerical experiments comparing the efficiency of sampling distributions that are based on ϵ -net to grids are presented in Section VI. We summarize our work and discuss future directions in Section VII.

II. RELATED WORK

We provide a literature review of results concerning the theoretical properties of PRM, where the majority of results apply to the setting consisting of a Euclidean configuration spaces, and samples that are generated in a uniform and random fashion.

The first theoretical analysis of PRM was obtained in [12]. It was shown that a PRM with n samples and fixed connection radius $r > 0$ will find a feasible solution, assuming that one exists with non-zero clearance, with probability at least $1 - ae^{-br^2n}$ for some constants $a, b > 0$. A measure theoretic analysis achieving similar results was developed in [13].

The celebrated work by Karaman and Frazzoli [15] initiated the study of asymptotic optimality in sampling-based planning. In the context of PRM, this paper proves that if $r > \gamma \left(\frac{\log n}{n}\right)^{1/d}$, for some constant $\gamma > 0$, then the length of the solution returned by PRM with high probability converges asymptotically almost surely, as the number of samples $n \rightarrow \infty$, to length cost of the robust optimal solution (i.e. the stretch factor of PRM converges to 1 a.a.s.). Such a connection radius leads to a graph of size $\Theta(n \log n)$, in contrast to a size

arXiv:1909.06363v1 [cs.DS] 13 Sep 2019

of $\Theta(n^2)$ induced by a constant radius (as in [1]). A finite-time analysis of PRM, providing probabilistic bounds for achieving a given stretch factor $1 + \epsilon$ for a fixed number of samples n and a specific connection radius of the aforementioned form was established in [18], [19].

Subsequent work has managed to further reduce the constant γ [7], [20]. A recent paper [21] establishes the existence of a critical connection radius $r^* = \gamma' \left(\frac{1}{n}\right)^{1/d}$, where γ' is constant: if $r < r^*$ then PRM is guaranteed to fail (even when $n \rightarrow \infty$), and if $r > r^*$ then it is guaranteed to converge a.a.s. to a near-optimal solution.

All the aforementioned theoretical results assume a uniform random sampling scheme. A recent work [17] establishes that using a low-dispersion deterministic sampling-schemes (e.g., Halton and Sukharev sequences), asymptotic optimality can be achieved with a radius as small as $f(n) \left(\frac{1}{n}\right)^{1/d}$, where $f(n)$ is any function such that $\lim_{n \rightarrow \infty} f(n) = \infty$.

Two recent works [22], [23] consider a non-Euclidean control-affine robotic systems and develop sufficient conditions for asymptotic optimality, with respect to the magnitude of r , and assuming random sampling and $n \rightarrow \infty$.

Non-uniform sampling algorithms have recently been proposed and improve sample efficiency by leveraging domain knowledge of typical motion planning environments [24], [25]. This methodology addresses average case complexity by constructing distributions over likely problem instances and is thus complementary to the worst case analysis that we study here.

III. PRELIMINARIES

We provide several basic definitions that will be used throughout the paper. Given two points $x, y \in \mathbb{R}^d$, denote by $\|x - y\|_p := \left(\sum_{i=1}^d |x_i - y_i|^p\right)^{1/p}$ the ℓ_p distance between them. When $p = 2$ we obtain the standard Euclidean distance. We denote the d -dimensional ℓ_p ball with radius $r > 0$ centered at $x \in \mathbb{R}^d$ as $B_p(x, r) := \left\{y : \|x - y\|_p \leq r\right\}$. For a Euclidean set \mathcal{X} we use $\text{co}(\mathcal{X})$ to denote its convex hull and $\text{vol}(\mathcal{X})$ to denote its volume (i.e. Lebesgue measure).

A. Motion planning

Denote by \mathcal{C} the configuration space of the robot, which, by rescaling we will assume is $[0, 1]^d$ throughout this paper. The free space $\mathcal{F} \subset \mathcal{C}$ denotes all collision-free configurations. A motion-planning problem is then specified by the tuple $(\mathcal{F}, x_{\text{start}}, x_{\text{goal}})$. The objective is to find a (continuous) path $p : [0, 1] \rightarrow [0, 1]^d$ that a) moves the robot from the start to goal location, i.e. $p(0) = x_{\text{start}}, p(1) = x_{\text{goal}}$ and b) avoids collisions with obstacles, i.e. $p(t) \in \mathcal{F}$ for all $t \in [0, 1]$.

It is usually desirable to obtain paths that minimize a given criterion. In this paper we measure the quality of a path p by its length $\ell(p)$. A crucial property of paths in sampling-based planning is the notion of clearance. We say that a motion-planning problem $(\mathcal{F}, x_{\text{start}}, x_{\text{goal}})$ has δ -clearance if there exists a path $p : [0, 1] \rightarrow [0, 1]^d$ with $p(0) = x_{\text{start}}, p(1) = x_{\text{goal}}$, and $\bigcup_{t \in [0, 1]} B_2(p(t), \delta) \subset \mathcal{F}$.

B. Probabilistic Roadmaps

We provide a formal definition of the Probabilistic Roadmaps Method (PRM). For a given motion-planning problem $\mathcal{M} := (\mathcal{F}, x_{\text{start}}, x_{\text{goal}})$, PRM generates a graph $G_{\mathcal{M}}$, whose vertices and edges represent collision-free configurations and

straight-line paths connecting configurations, respectively. The motivation behind this construction is to yield a connected component of $G_{\mathcal{M}}$, which contains x_{start} and x_{goal} , and thus induces a collision-free path connecting the two configurations.

The PRM graph induced by $\mathcal{M}, \mathcal{X}, r$ is denoted by $G_{\mathcal{M}}(\mathcal{X}, r) = (V, E)$. The vertices V consist of all collision-free configurations in $\mathcal{X} \cup \{x_{\text{start}}, x_{\text{goal}}\}$. The (undirected) edges E connect between every pair of vertices $u, v \in V$ such that (i) the distance between them is at most r , and (ii) the straight-line path between them is entirely collision free. Formally,

$$V := (\mathcal{X} \cup \{x_{\text{start}}, x_{\text{goal}}\}) \cap \mathcal{F},$$

$$E := \{(u, v) \in V \times V : \|u - v\|_2 \leq r, \text{co}(\{u, v\}) \subset \mathcal{F}\}.$$

C. Sampling distributions

The choice of sample set \mathcal{X} has significant implications on the properties of $G_{\mathcal{M}}(\mathcal{X}, r)$. For this reason, we discuss two types of sample sets, namely ϵ -nets and grids, that are particularly useful for PRM. Throughout this paper we will use *sample set* and *sample distribution* interchangeably when referring to \mathcal{X} .

Definition 1 (ϵ -nets). A set $\mathcal{B} \subset \mathbb{R}^d$ is a ϵ -net for a set $\mathcal{A} \subset \mathbb{R}^d$ if for every $a \in \mathcal{A}$, there exists a $b \in \mathcal{B}$ so that $\|a - b\|_2 \leq \epsilon$.

As far as motion planning is concerned, ϵ -nets are good candidates for deterministic sampling schemes since by definition they have uniformly dense coverage over the entire space. The low dispersion sequences mentioned in [17] (i.e. Sukharev Grids) are special cases of ϵ -nets, and we will show that studying these objects in full generality leads to improved covering efficiency. *Minimal* ϵ -nets, i.e. nets with the smallest possible cardinality, are then good candidates for *efficiently* covering the entire space. We will make these intuitions formal in the coming sections. Grids have long seen use as sample sets in motion planning [26], so we use grids as benchmarks against which we compare the performance of sample sets inspired by ϵ -nets. We define a Sukharev grid of $[0, 1]^d$ with spacing w to be the following collection of points:

$$\mathcal{X}_{\text{grid}}(w) := \left\{x \in \mathbb{R}^d : \frac{x_i}{w} + \frac{1}{2} \in \left\{1, 2, \dots, \frac{1}{w}\right\} \forall i\right\}.$$

From this point onward we refer to $\mathcal{X}_{\text{grid}}(w)$ as a grid with spacing w . See Section IV-C for a detailed comparison between grid sampling and ϵ -net sampling.

D. Completeness as a Benchmark

To state our main objectives, we will use the following benchmark to measure the quality of samples set \mathcal{X} and a connection radius.

Definition 2 ((δ, ϵ) -completeness). Given a samples set \mathcal{X} and a connection radius r , we say that the pair (\mathcal{X}, r) is (δ, ϵ) -complete if for every δ -clear \mathcal{M} it holds that

$$d_{G_{\mathcal{M}}(\mathcal{X}, r)}(x_{\text{start}}, x_{\text{goal}}) < (1 + \epsilon) \cdot \text{OPT}_{\delta},$$

where $d_{G_{\mathcal{M}}(\mathcal{X}, r)}(x_{\text{start}}, x_{\text{goal}})$ denotes the length of the shortest path from start to goal in the graph $G_{\mathcal{M}}(\mathcal{X}, r)$, and OPT_{δ} is the length of the shortest δ -clear solution to \mathcal{M} .

Note that $\epsilon = \infty$ corresponds to the case where finding a feasible (though not necessarily high quality) path is the only objective.

IV. SAMPLE COMPLEXITY OF PRM

Our main objective in this work is to study the sample complexity of PRM. For a clearance level $\delta > 0$ and a stretch tolerance $\epsilon > 0$, we wish to which combinations of a sample set \mathcal{X} and radius r guarantee (δ, ϵ) -completeness. The properties of ϵ -nets are central to our contributions to both of these goals, as well as our experimental results in Section VI.

We focus on deterministic sampling since our techniques can be used to derive results for i.i.d. sampling procedures as well, which show a poorer performance of i.i.d. sampling, in line with the findings of [17]. As required by our main objectives, all of the results presented here are presented in the finite-sample, non-asymptotic setting.

We will prove sufficient conditions on sample complexity in a constructive way by exhibiting algorithms that achieve the conditions. To this end, the **Epsilon Net Sampling** (ENS) procedure presented in Algorithm 2 will be used to certify the sufficient conditions. ENS leverages properties of ϵ -nets to determine a connection radius r and net resolution δ_{\min} . It then calls as a subroutine the **Build-Net** algorithm, which constructs a δ_{\min} -net of the configuration space by including points until a δ_{\min} -net is obtained, while ensuring that all points included are at pairwise distance at least δ_{\min} . In the next sections, we will prove the efficacy of ENS which in turn gives sufficient conditions on the complexity of PRM.

Algorithm 1: Build-Net

1 **Input:** Set \mathcal{A} , cover radius $\epsilon > 0$;
2 **Output:** An ϵ -net \mathcal{B} for \mathcal{A} ;
3 $\mathcal{B} \leftarrow \emptyset$;
4 **while** $\mathcal{A} \setminus \cup_{b \in \mathcal{B}} B_2(y, \epsilon) \neq \emptyset$ **do**
5 Find $y \in \mathcal{A} \setminus \cup_{b \in \mathcal{B}} B_2(b, \epsilon)$;
6 $\mathcal{B} \leftarrow \mathcal{B} \cup \{y\}$;
7 **return** \mathcal{B} .

Algorithm 2: Epsilon Net Sampling (ENS)

1 **Input:** Sample size n , workspace dimension d , stretch tolerance $\epsilon > 0$, δ clearance parameter;
2 **Output:** Sample set \mathcal{X} and connection radius r ;
3 $\alpha \leftarrow \frac{\epsilon}{\sqrt{1+\epsilon^2}}$;
4 $n_\delta \leftarrow \min \left\{ \sqrt{\pi d} \left(\sqrt{\frac{2d}{\pi e}} \cdot \frac{1-(2-\alpha)\delta}{\alpha\delta} \right)^d, n \right\}$;
5 $\delta_{\min} \leftarrow \sqrt{\frac{2d}{\pi e}} \left(\frac{\sqrt{\pi d}}{n_\delta} \right)^{\frac{1}{d}} \left[\alpha - (2-\alpha) \sqrt{\frac{2d}{\pi e}} \left(\frac{\sqrt{\pi d}}{n_\delta} \right)^{\frac{1}{d}} \right]^{-1}$;
6 $r \leftarrow 2 \left(\alpha + \sqrt{1-\alpha^2} \right) \delta_{\min}$;
7 $\mathcal{X} \leftarrow \text{Build-Net}([\delta_{\min}, 1 - \delta_{\min}]^d, \delta_{\min})$;
8 **return** (\mathcal{X}, r) .

A. Sample complexity

In this section we make progress on characterizing the sample complexity of PRM, that is when does a samples set \mathcal{X} guarantee (δ, ϵ) -completeness, and when it does not. The following theorem provides a necessary condition on the size of the sample set $n = |\mathcal{X}|$ and radius r .

Theorem 1 (Necessary Conditions). *Let $\mathcal{X} \subset [0, 1]^d$ be a set of n points and let $\delta > 0$. If (\mathcal{X}, r) is (δ, ∞) -complete then*

$$n \geq \sqrt{\frac{e}{2}} \left(1 - \frac{2\delta}{1-2\delta} \right)^2 \left(\sqrt{\frac{d-1}{2\pi e}} \cdot \frac{(1-2\delta)}{\delta} \right)^d$$

$$\text{and } r \geq (1-2\delta) \left(\sqrt{\pi d} \right)^{1/d} \sqrt{\frac{d}{2\pi e}} \left(\frac{1}{n} \right)^{1/d}.$$

In particular, any sample set of size less than the lower bound, regardless of r and how the points are chosen, cannot yield be (δ, ∞) -complete. With this result in place, we now focus our efforts in finding (\mathcal{X}, r) with size and radius comparable to the lower bound from Theorem 1, for which (δ, ϵ) -completeness is guaranteed. The following theorem leverages ENS to achieve this goal.

Theorem 2 (Sufficient Conditions). *Let $\epsilon > 0, \delta > 0$. If*

$$n \geq \sqrt{\pi d} \left(\sqrt{\frac{2d}{\pi e}} \cdot \frac{1-(2-\alpha)\delta}{\alpha\delta} \right)^d \text{ and}$$

$$r \geq 2 \left(1 + \frac{1}{\epsilon} \right) \left(\sqrt{\pi d} \right)^{1/d} \sqrt{\frac{d}{2\pi e}} \left(\frac{1}{n} \right)^{1/d}$$

where $\alpha = \frac{\epsilon}{\sqrt{1+\epsilon^2}}$, then $(\mathcal{X}, r) = \text{ENS}(n, d, \delta)$ is (δ, ϵ) -complete.

See Sections VIII-A and VIII-B for proofs of Theorems 1 and 2.

B. Discussion

A few comments are in order. The connection radius condition in Theorem 2 generalizes the works of [15] and [17] to finite sample settings. Concretely, choosing $\epsilon = (\log n)^{-1/d}$ achieves asymptotic optimality with a radius $r = \gamma \left(\frac{\log n}{n} \right)^{1/d}$, recovering the result of [15]. This is because $\epsilon \rightarrow 0$ as $n \rightarrow \infty$, and the minimum δ satisfying the sample condition in Theorem 2 goes to zero as $n \rightarrow \infty$. More generally, for any diverging function $f(n)$, choosing $\epsilon = \frac{1}{f(n)}$ recovers the asymptotic optimality condition $r = \gamma f(n) n^{-1/d}$ from [17].

Theorem 2 provides several other additions to the motion planning literature. It provides guarantees on stretch factor achievable with finite n , which are not specified in the aforementioned works. This result is actionable in the sense that if δ is known and ϵ is specified, then it gives a sample size and distribution that is guaranteed to find a solution with the desired quality. Conversely, Theorem 2 can be used as a certificate of hardness (or as a non-existence proof [27], [28]): for any $n, \delta > 0$ satisfying the condition in Theorem 2, if there does not exist a feasible path in $\mathcal{G}_{\mathcal{M}}(\mathcal{X}, r)$ where $(\mathcal{X}, r) = \text{ENS}(n, d, \delta)$, then it must be the case that \mathcal{M} has clearance strictly less than δ .

We now discuss the implications of our results on the sample complexity of PRM. For small dimensions, i.e., $d \leq 4$, Theorem 2 shows that $O(\delta^{-d})$ samples are sufficient to achieve (δ, ∞) -completeness, since $\epsilon = \infty$ corresponds to $\alpha = 1$. Conversely, Theorem 1 shows that this sample complexity is essentially optimal (i.e. up to a multiplicative constant factor) in the sense that every (δ, ∞) -complete (\mathcal{X}, r) must have $|\mathcal{X}| = \Omega(\delta^{-d})$.

In high dimensions, note that the ratio between the sufficient and necessary conditions on sample size is $\Omega(2^d \sqrt{d})$. Thus when d is no longer a small constant, there is a significant gap between the achievability result of Theorem 2 to the lower bound on sample complexity given by Theorem 1.

Evaluating the Bounds: To give a sense of the sample size conditions specified by Theorems 1 and 2, Table I evaluates bounds for $n = |\mathcal{X}|$ with respect various values of δ, d, ϵ .

From this we observe a poor scaling with clearance level δ , implying that PRM with classical sampling methods is likely not the right tool for high dimensional, low clearance motion-planning problems with low error tolerance (i.e., where success must be guaranteed). For example, if \mathcal{M} is a maze in $d = 5$ dimensions with path width 0.01 (i.e. clearance $\delta = 0.005$), then by Theorem 1, at least $9.2 \cdot 10^9$ samples are needed to ensure that PRM will find a solution to the maze. A graph this size is beyond what can be stored by modern computers.

The story is more optimistic for larger values of δ (i.e., problems with higher clearance) and lower dimensions. When $\delta = 0.25$, a feasible solution can be guaranteed (see $\epsilon = \infty$) by using around 8000 samples. For $d = 4, \delta = 0.1$, a feasible solution can be guaranteed with 20,000 samples. In fact, a stretch factor of 2 (see $\epsilon = 1$) can be guaranteed in $\delta = 0.25$ clearance with a similar sample size on the order of 10^4 . Theorem 2 reveals that, with the right sampling scheme, PRM is guaranteed to find a solution efficiently and can do so in real time. For smaller clearance levels like $\delta = 0.1$, a solution can be guaranteed by using somewhere between 10^5 and 10^6 samples, depending on the dimension. A solution with stretch factor 2 can be guaranteed by inflating the sample size by an additional factor of 10. This is no longer acceptable for real-time applications, but is still manageable for offline preprocessing if the environment will be queried many times, allowing for a cheap amortized cost.

While many practical robotic systems are high dimensional, i.e., $d \geq 6$, some application instances naturally admit decoupling of the degrees of freedom of the system, which induces lower-dimensional configuration subspaces. For instance, manipulation problem (see, e.g., [2]) can be typically decomposed into a sequence of tasks where the manipulator is driving toward an object (while fixing its arms), then moves an arm towards the object, and finally grasps it by actuation its fingers. Additionally, in some settings which exploit learning-based techniques, sampling of a lower-dimensional subspace can inform sampling in the full configuration space, which can lead to more informative sampling distributions [29], [30].

Table I
SAMPLE COMPLEXITY EXAMPLES

| δ | d | Thm. 1 LB | Thm. 2 UB | | |
|----------|-----|-------------------|---------------------|-------------------|---------------------|
| | | | $\epsilon = \infty$ | $\epsilon = 1$ | $\epsilon = 0.25$ |
| 0.25 | 4 | 0 | 252 | 669 | 22737 |
| 0.25 | 5 | 0 | 1430 | 4837 | $3.9 \cdot 10^5$ |
| 0.25 | 6 | 0 | 8781 | 37930 | $7.5 \cdot 10^6$ |
| 0.1 | 4 | 82 | 20411 | $7.15 \cdot 10^4$ | $4.2 \cdot 10^6$ |
| 0.1 | 5 | 570 | $3.48 \cdot 10^5$ | $1.66 \cdot 10^6$ | $2.6 \cdot 10^8$ |
| 0.1 | 6 | 4313 | $6.41 \cdot 10^6$ | $4.19 \cdot 10^7$ | $1.8 \cdot 10^{10}$ |
| 0.05 | 4 | 2983 | $4.1 \cdot 10^5$ | $1.52 \cdot 10^6$ | $9.9 \cdot 10^7$ |
| 0.05 | 5 | 46201 | $1.46 \cdot 10^7$ | $7.62 \cdot 10^7$ | $1.4 \cdot 10^{10}$ |
| 0.05 | 6 | $7.86 \cdot 10^5$ | $5.67 \cdot 10^8$ | $4.13 \cdot 10^9$ | $2.2 \cdot 10^{12}$ |

C. Implications for Grid Sampling

The achievability result from Theorem 2 is obtained by constructing an algorithm, namely **ENS**, which has the desired properties. In this section we provide sufficient condition on sample size for PRM to be (δ, ϵ) -complete when using grid sampling. Such a result serves as a benchmark for the proposed sampling algorithm **ENS**, and may be of independent interest as grids are commonly used in motion planning.

Corollary 1 (Sufficient Condition for Grid Sampling). *Take r to satisfy the connection radius condition given in Theorem 2. Then $(\mathcal{X}_{\text{grid}}(\frac{2\alpha\delta}{\sqrt{d}}), r)$ is (δ, ϵ) -complete and*

$$|\mathcal{X}_{\text{grid}}(\frac{2\alpha\delta}{\sqrt{d}})| = \left(\frac{\sqrt{d}}{2} \cdot \frac{1-2\delta}{\alpha\delta}\right)^d, \text{ where } \alpha = \frac{\epsilon}{\sqrt{1+\epsilon^2}}.$$

See Section IX-C for a proof of corollary 1.

Grids have long seen use in sampling based motion planning problems. One natural comparison to make then is between the quality of coverage offered by grids versus ϵ -net approaches like **Build-Net**. A high resolution grid is in fact an example of an ϵ -net. There is, however, one key distinction between a grid and general ϵ -nets. Technically, a grid is a covering of the space using ℓ_∞ balls, whereas ϵ -nets provide coverings via ℓ_2 balls. Grids obtain their status as ϵ -nets through norm equivalence, i.e. $\|x\|_\infty \leq \|x\|_2 \leq \sqrt{d}\|x\|_\infty \forall x \in \mathbb{R}^d$. The ℓ_2 norm is more prevalent than ℓ_∞ in the motion planning literature as δ -clearance and connection radius conditions are both stated with respect to Euclidean distance. It stands to reason that general ϵ -nets would provide a more efficient sampling strategy for motion planning problems and algorithms that are specified by ℓ_2 distance. Corollary 1 providing a worse (i.e. larger) sufficient condition than Theorem 2 corroborates this intuition. Furthermore, in this section we show that, under the condition $\epsilon < \sqrt{\frac{\pi\epsilon}{8}} - 1 \approx 0.033$, there exist ϵ -nets that are asymptotically (as $\epsilon \rightarrow 0, d \rightarrow \infty$) more efficient than grids when it comes to covering the space with ℓ_2 balls.

Lemma 1 (Net size and Grid size). *$\mathcal{X}_{\text{grid}}(w)$ is an ϵ -net if and only if $w \leq \frac{2\epsilon}{\sqrt{d}}$, thus the smallest grid that is also an ϵ -net is $\mathcal{X}_{\text{grid}}(\frac{2\epsilon}{\sqrt{d}})$. If \mathcal{X} is an ϵ -net obtained from **Build-Net** $([0, 1]^d, \epsilon)$, then we have*

$$\frac{|\mathcal{X}|}{|\mathcal{X}_{\text{grid}}(\frac{2\epsilon}{\sqrt{d}})|} \leq \sqrt{\pi d} \left(\frac{\sqrt{8}(1+\epsilon)}{\sqrt{\pi\epsilon}}\right)^d.$$

See Section IX-B for a proof of Lemma 1. When $\epsilon < \sqrt{\frac{\pi\epsilon}{8}} - 1$ we have $\frac{\sqrt{8}(1+\epsilon)}{\sqrt{\pi\epsilon}} < 1$, hence the ratio given by Lemma 1 goes to zero as $d \rightarrow \infty$. We can then conclude that there exist ϵ -nets that are more efficient than grids for high dimensional problems. For lower dimensions, the upper bound from Lemma 1 is larger than 1. We suspect however, that the bound is loose in this regime and that ϵ -nets remain competitive with grids even for small dimensions. To test our hypothesis, we conduct an empirical comparison between ϵ -net inspired sample sets and grids in Section VI.

For some intuition as to why ϵ -nets provide more efficient coverage than grids in high dimensions, we note that Algorithm 1 returns an ϵ -net \mathcal{X} whose points are pairwise at distance at least ϵ . The grid on the other hand, has spacing at

most $\frac{2\epsilon}{\sqrt{d}}$. The shrinkage factor of $O\left(\frac{1}{\sqrt{d}}\right)$ is precisely from the error in approximating ℓ_2 by ℓ_∞ . Since the minimum separation in the grid is smaller, the balls in $\cup_{x \in \mathcal{X}_{\text{grid}}(2\epsilon/\sqrt{d})} B_2(x, \epsilon)$ overlap more than the balls in $\cup_{x \in \mathcal{X}} B_2(x, \epsilon)$ and thus lead to less efficient coverage.

V. PROOF SKETCHES

In this section we sketch the proofs of the sample size conditions in Theorems 1 and 2. To set the stage, we first discuss the cardinality of minimal ϵ -nets, which play a key role in the proofs. The following result provides upper and lower bounds on the size of minimal nets.

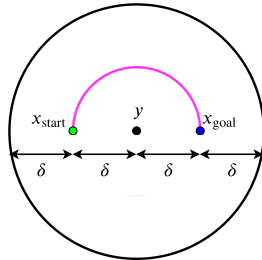
Theorem 3 (Cardinality of epsilon nets). *Let $\mathcal{A} \subset \mathbb{R}^d$ be a set.*

- 1) Every ϵ -net of \mathcal{A} must have cardinality at least $\text{vol}(\mathcal{A}) \sqrt{\pi d} \left(\sqrt{\frac{d}{2\pi e}} \frac{1}{\epsilon} \right)^d$.
- 2) There exists a ϵ -net of \mathcal{A} with cardinality at most $\text{vol}(\mathcal{A} \oplus B_2(y, \frac{\epsilon}{2})) \sqrt{\pi d} \left(\sqrt{\frac{2d}{\pi e}} \frac{1}{\epsilon} \right)^d$.

Where $A \oplus B := \{a + b : a \in A, b \in B\}$ denotes the Minkowski sum of the sets \mathcal{A} and \mathcal{B} . Theorem 3 is well established result in the learning theory and statistics communities, but for completeness we provide a proof in Section IX-A. The **Build-Net** procedure outlined by Algorithm 1 is one particular way to generate an ϵ -net with property 2 of Theorem 3.

A. Proof Sketch for Theorem 1

The outline for the proof sketch is by as follows. (1) Suppose the sample set $\{x_i\}_{i=1}^n$ has $n < \sqrt{\pi d} \left(\sqrt{\frac{d}{2\pi e}} \frac{1-4\delta}{2\delta} \right)^d$. (2) By part 1 of Theorem 3, $\{x_i\}_{i=1}^n$ cannot be a 2δ -net of $[2\delta, 1-2\delta]^d$. (3) This means that there exists some y so that $\{x_i\}_{i=1}^n \cap B_2(y, 2\delta) = \emptyset$, i.e. it is empty. Furthermore, since $y \in [2\delta, 1-2\delta]^d$, we have $B_2(y, 2\delta) \subset [0, 1]^d$. (4) Consider the motion planning problem $\mathcal{M} := (\mathcal{F}, x_{\text{start}}, x_{\text{goal}})$: The black dot is y , $x_{\text{start}} = y - \delta e_1$, $x_{\text{goal}} = y + \delta e_1$ ($\{e_i\}_{i=1}^d$ are the standard basis vectors for \mathbb{R}^d .) depicted by the green and blue dots respectively, and obstacle set $\mathcal{F} := \{y\} \cup \{x : \|x - y\|_2 = 2\delta\}$ shown in black. This problem is δ -clear, and a solution trajectory is shown in pink. There is, however, no way to reach x_{start} from x_{goal} in $G_{\mathcal{M}}$. This is because the obstacle $\{y\}$ blocks the edge between x_{start} and the x_{goal} , and the shell $\{x : \|x - y\|_2 = 2\delta\}$ blocks any edges from these points to all points $\{x_i\}_{i=1}^n$. Thus, the nodes $x_{\text{start}}, x_{\text{goal}}$ will have no neighbors in $G_{\mathcal{M}}$. We conclude that, regardless of the value of r , no sample set of size $n < \sqrt{\pi d} \left(\sqrt{\frac{d}{2\pi e}} \frac{1-4\delta}{2\delta} \right)^d$ can be (δ, ∞) -complete in $[0, 1]^d$. The proof of Theorem 1 uses this idea but packs the space using a torus instead of a ball. Since a similar argument can be done using the torus, and the torus used has smaller volume than the ball, more tori can be packed, leading to a larger lower bound.



B. Proof Sketch for Theorem 2

Suppose \mathcal{M} is a δ_{min} -clearance motion planning problem for some $\delta_{\text{min}} > 0$. It then has a shortest δ_{min} -clear solution path p . Consider points $\{p_j\}_{j=1}^m$ on the path p so that consecutive points are at $2\sqrt{1-\alpha^2}\delta_{\text{min}}$ euclidean distance apart. See Fig. 1 for an illustration. For each $1 \leq j \leq m-1$, by δ_{min} -clearance the balls of radius δ_{min} centered at p_j, p_{j+1} are collision free. This is illustrated by the blue region in Fig. 1. If we have a collection of samples \mathcal{X} which forms a $\alpha\delta_{\text{min}}$ -net of the space, then we are guaranteed that there are $z_j, z_{j+1} \in \mathcal{X}$ that are within $\alpha\delta_{\text{min}}$ distance of p_j and p_{j+1} respectively. This is illustrated by the green regions. The condition on n given in the statement of Theorem 2 in conjunction with Theorem 3 guarantees the existence of such a \mathcal{X} . The spacing $2\sqrt{1-\alpha^2}\delta_{\text{min}}$ was chosen so that the convex hull of the green set, depicted as the union of the green and violet regions, is entirely contained in the blue, collision free region. This means that any line segment joining a point in the left green ball to a point in the right green ball is collision-free. Therefore, for each j , the line segment joining z_j to z_{j+1} is collision-free for every $1 \leq j \leq m-1$. Furthermore, by triangle inequality, the length of these segments can be at most $2(\alpha + \sqrt{1-\alpha^2})\delta_{\text{min}}$. Thus, if we choose r to be this value, then the edges $\{(z_j, z_{j+1})\}_{j=1}^{m-1}$ will all be in the graph $G_{\mathcal{M}}(\mathcal{X}, r)$. Since p is a solution path, we can choose the first and last samples $p_1 = x_{\text{start}}$ and $p_m = x_{\text{goal}}$. Therefore the path that concatenates these edges will be a collision-free path from the start to the goal in the graph $G_{\mathcal{M}}(\mathcal{X}, r)$. Finally, to bound the length of this path, note that the length of the path from p_j to p_{j+1} is at least $\|p_j - p_{j+1}\|_2 = 2\sqrt{1-\alpha^2}\delta_{\text{min}}$. We then have

$$\frac{\|z_j - z_{j+1}\|_2}{\|p_j - p_{j+1}\|_2} \leq \frac{2(\alpha + \sqrt{1-\alpha^2})\delta_{\text{min}}}{2\sqrt{1-\alpha^2}\delta_{\text{min}}} = 1 + \frac{\alpha}{\sqrt{1-\alpha^2}} = 1 + \epsilon$$

where the last equality is due to the definition of α . Since each piece of the path defined by $\{z_j\}_{j=1}^m$ is not more than $1 + \epsilon$ times its corresponding piece in p , this gives a path whose total length is at most $1 + \epsilon$ times the length of p .

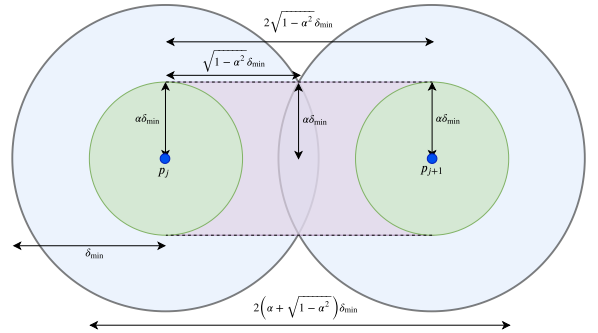


Figure 1. A visualization of the proof technique of Theorem 2 in 2 dimensions.

VI. EXPERIMENTS

In this section we demonstrate the improved efficiency of sampling methods that are based on ϵ -nets, compared to grids. While Lemma 1 shows that ϵ -nets are provably more efficient than grids asymptotically as $d \rightarrow \infty$, it does not

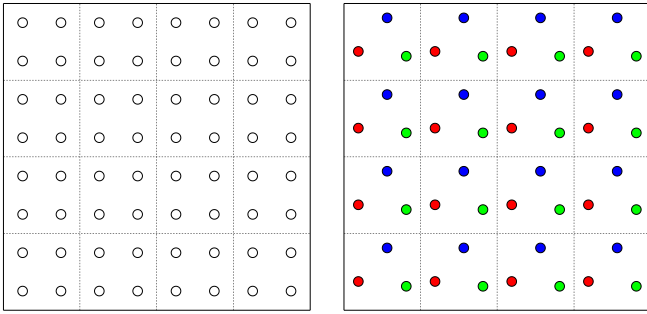


Figure 2. **Left:** A grid of width 8 in $d = 2$ dimensions can be represented by repeating a grid of width 2 a total of 16 times. **Right:** More generally, any $\mathcal{T} := (x_1, x_2, x_3)$ which forms an ϵ -net of $[0, \frac{1}{4}]^2$ can be replicated 16 times to attain an ϵ -net of $[0, 1]^2$.

address the comparison in low dimensions when d is small. To make an empirical comparison in the non-asymptotic regime, we numerically construct sample sets based on ϵ -nets and compare their size and coverage quality to grids. This section is organized as follows. In Section VI-A we introduce a sampling method inspired by ϵ -nets, describe the experimental design and how we plan on comparing the proposed sampling method to grids. We present the results of our experiments in Section VI-B, and have a discussion on the results in Section VI-C.

A. The Sampling Procedure

When ϵ is small, it is computationally expensive to find a cover of the space with balls of radius ϵ . To alleviate this computational burden, we make the following observation. Suppose \mathcal{T} is a ϵ -net of $[0, m^{-1}]^d$. Since $[0, 1]^d$ can be written as a union of m^d translations of $[0, m^{-1}]^d$, the union of the analogous m^d translates of \mathcal{T} gives an ϵ -net of $[0, 1]^d$. Grids are in fact one example of ϵ -nets with this periodic structure. See Fig. 2 for an example in $d = 2$ dimensions. If instead we want a $\epsilon/2$ net, we can replicate $\frac{1}{2}\mathcal{T}$ a total of $(2m)^d$ times. For this reason, we call \mathcal{T} a *template*, since scaling it and replicating it appropriately can create ϵ -nets of arbitrary resolution and size. Since the templates can be rescaled and replicated to create ϵ -nets of arbitrary resolution and size, they can be computed offline, since rescaling and replication is computationally cheap and can be done online. Due to this versatility, it is acceptable for the computation of these templates to be expensive, since the templates can also be shared among practitioners.

With this in mind our goal is to find templates of small cardinality for a large range of problem dimensions. Our benchmark will be a grid with spacing $w := \frac{2\epsilon}{\sqrt{d}}$, since we showed in Lemma 1 that a grid is an ϵ -net if and only if its spacing is at most w . The cube $[0, kw]^d$ is covered by a grid of spacing w with exactly k^d points. See Fig. 2 for a 2D example. Thus our goal is to find a ϵ -net of $[0, kw]^d$ with fewer than k^d points. This problem is homogeneous in ϵ , so by re-scaling, this is equivalent to finding a $\frac{\sqrt{d}}{2k}$ -cover of $[0, 1]^d$ using fewer than k^d points. Moreover, since grids themselves are periodic, the ratio of sizes of the sample set obtained by repeating \mathcal{T} to the grid will also be $|\mathcal{T}|/k^d$.

Certifying that a template \mathcal{T} is a $\frac{\sqrt{d}}{2k}$ -net of $[0, 1]^d$ is nontrivial because there are infinitely many conditions to

satisfy, i.e. each $x \in [0, 1]^d$ must be at distance at most $\frac{\sqrt{d}}{2k}$ from \mathcal{T} . Sufficient conditions involving only finitely many constraints can be derived using triangle inequality, but in practice we found these methods to be too conservative. We instead densely sample a large collection of points uniformly at random from $[0, 1]^d$, denoted \mathcal{V} , and obtain a $\frac{\sqrt{d}}{2k}$ -net of those points via the output of `Build-Net`($\mathcal{V}, \frac{\sqrt{d}}{2k}$). The resulting set of points \mathcal{T} may not be a $\frac{\sqrt{d}}{2k}$ -net of $[0, 1]^d$ since it is only certified to be a net of the set of densely sampled points. We say a point is uncovered by \mathcal{T} if its nearest neighbor in \mathcal{T} is at distance more than $\frac{\sqrt{d}}{2k}$. To address this detail, we verify using Monte Carlo simulation that only a negligible fraction of $[0, 1]^d$ is uncovered by \mathcal{T} .

B. Numerical Results

We created templates \mathcal{T} using the procedure described in the previous section for various values of dimension d and k . We recorded the size of the resulting template, as well as the empirical estimate \hat{p} on the volume of uncovered space. For each trial, \hat{p} was computed via Monte Carlo with 10 million samples. The ratio between $|\mathcal{T}|$ and the size of the grid benchmark, k^d , is denoted as ρ . An efficient sample set \mathcal{T} will lead to a small value of ρ . Table II summarizes the results of this experiment.

Table II
TEMPLATE SIZES FOR VARIOUS DIMENSIONS

| d | $k = 2$ | | | $k = 3$ | | |
|-----|-----------------|--------|---------------------|-----------------|--------|---------------------|
| | $ \mathcal{T} $ | ρ | \hat{p} | $ \mathcal{T} $ | ρ | \hat{p} |
| 4 | 15 | 0.93 | $3.7 \cdot 10^{-2}$ | 77 | 0.95 | $1.4 \cdot 10^{-2}$ |
| 5 | 27 | 0.84 | $3.3 \cdot 10^{-2}$ | 189 | 0.77 | $5.7 \cdot 10^{-3}$ |
| 6 | 57 | 0.89 | $5.5 \cdot 10^{-3}$ | 457 | 0.63 | $2.4 \cdot 10^{-3}$ |
| 7 | 105 | 0.82 | $3.1 \cdot 10^{-3}$ | 1078 | 0.50 | $1.4 \cdot 10^{-3}$ |
| 8 | 173 | 0.68 | $1.6 \cdot 10^{-3}$ | 2477 | 0.38 | $6.4 \cdot 10^{-4}$ |
| 9 | 291 | 0.58 | $1.3 \cdot 10^{-3}$ | 5650 | 0.29 | $2.6 \cdot 10^{-4}$ |

C. Discussion

From Table II we see that the relative efficiency compared to the grid, ρ , improves as the dimension grows. This observation is consistent with the asymptotic implications of Lemma 1. For all dimensions, the value of \hat{p} is on the order of 10^{-3} , which means that the templates are $\frac{\sqrt{d}}{2k}$ -nets of almost the entire space. Notice that the achieved value of ρ is better when $k = 3$ than when $k = 2$ across all tested dimensions. This is because the `Build-Net` procedure does not exploit the fact that \mathcal{T} will be used in a periodic manner. Simply put, there are covering inefficiencies at the boundaries when templates are used in a periodic manner. When covering $[0, 1]^d$ with larger templates, there are fewer boundaries between individual template replicas, and thus fewer instances where this boundary inefficiency exists. This reveals a natural trade-off between computation and sample efficiency. Indeed, the cover radius $\frac{\sqrt{d}}{2k}$ is a decreasing function of k , meaning it is more difficult computationally to find templates for larger k . Thus using small k is computationally cheap, but as Table II shows, the quality of the template is worse than what would be obtained for larger k . Looking at the extremes, $k = 1$ corresponds to the grid, and $k = \frac{\sqrt{d}}{2\epsilon}$ corresponds to finding an ϵ -net of $[0, 1]^d$ without exploiting templates or periodic translation in any way.

VII. CONCLUSION AND FUTURE WORK

In this paper we made progress in the characterization of sample complexity of PRM. We provided lower bounds on the sample size that is necessary for (δ, ϵ) -complete sampling algorithms. We then complemented the lower bound with achievability results by analyzing ϵ -net and grid based sampling schemes. These sampling schemes are then showed to attain, up to constant factors, the optimal sample and time complexity for lower dimensional problems. Through numerical experiments we exhibited a particular ϵ -net inspired sampling strategy, which we refer to as the template method, that offers nearly the same coverage quality as grids while using significantly fewer samples. The template method constructs sample sets of the space by appropriately rescaling and replicating a carefully chosen set of points (the template). Since rescaling and replicating is computationally cheap, and thus can be done online, the templates themselves can be computed offline and shared with practitioners to improve sample efficiency of PRM in practice.

There are several interesting directions for future research. First, the gap between the sufficient and necessary conditions for (δ, ϵ) -completeness provided here is dimension dependent. In high dimensions, the characterization is no longer tight, and the precise dependence of sample and time complexity on dimension is not yet known. In fact, the gap in our results is due to the gap in characterization of ϵ -net sizes in Theorem 3, thus closing that gap would have implications for our results. Second, while the templates proposed in our experiments show nearly the same coverage quality as grids, they may not be true ϵ -nets since they are only certified to be an ϵ -net of a large subset of the space. While we showed empirically that the volume of uncovered points is typically on the order of 10^{-3} , we would like to build templates that are certifiably ϵ -nets for the whole space while retaining reduced size observed in our experiments. Since Build-Net is used in both our theoretical and experimental results, a better algorithm for constructing ϵ -nets would lead to improved results both in theory and in practice.

REFERENCES

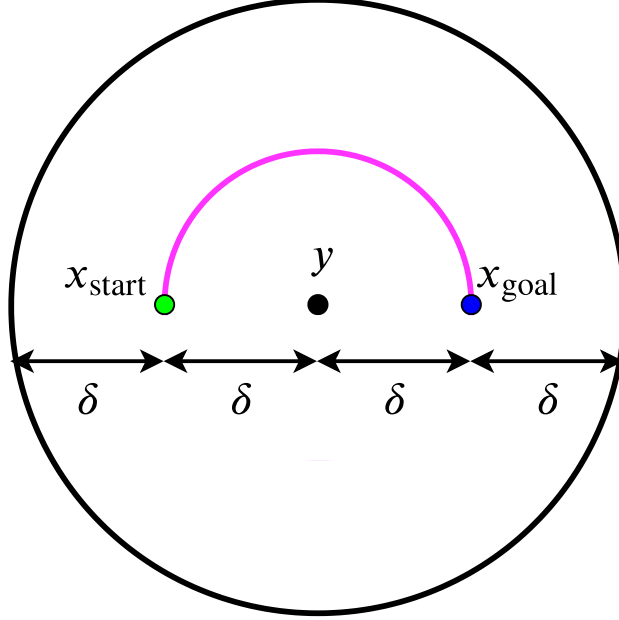
- [1] L. E. Kavraki, P. Svestka, J. Latombe, and M. H. Overmars, "Probabilistic roadmaps for path planning in high-dimensional configuration spaces," *IEEE Trans. Robotics and Automation*, vol. 12, no. 4, pp. 566–580, 1996. 1, 2
- [2] A. Kimmel, R. Shome, Z. Littlefield, and K. E. Bekris, "Fast, anytime motion planning for prehensile manipulation in clutter," in *18th IEEE-RAS International Conference on Humanoid Robots, Humanoids 2018, Beijing, China, November 6-9, 2018*, 2018, pp. 1–9. 1, 4
- [3] M. Fu, A. Kuntz, O. Salzman, and R. Alterovitz, "Toward asymptotically-optimal inspection planning via efficient near-optimal graph search," in *Robotics: Science and Systems*, Freiburg im Breisgau, Germany, 2019. 1
- [4] C. R. Garrett, T. Lozano-Pérez, and L. P. Kaelbling, "Ffrob: Leveraging symbolic planning for efficient task and motion planning," *I. J. Robotics Res.*, vol. 37, no. 1, pp. 104–136, 2018. 1
- [5] R. Shome, K. Solovey, A. Dobson, D. Halperin, and K. E. Bekris, "dRRT*: Scalable and informed asymptotically-optimal multi-robot motion planning," *Autonomous Robots*, Jan 2019. 1
- [6] W. Hönig, J. A. Preiss, T. K. S. Kumar, G. S. Sukhatme, and N. Ayanian, "Trajectory planning for quadrotor swarms," *IEEE Trans. Robotics*, vol. 34, no. 4, pp. 856–869, 2018. 1
- [7] L. Janson, E. Schmerling, A. A. Clark, and M. Pavone, "Fast marching tree: A fast marching sampling-based method for optimal motion planning in many dimensions," *International Journal of Robotics Research*, vol. 34, no. 7, pp. 883–921, 2015. 1, 2
- [8] J. A. Starek, J. V. Gómez, E. Schmerling, L. Janson, L. Moreno, and M. Pavone, "An asymptotically-optimal sampling-based algorithm for Bi-directional motion planning," in *IEEE/RSJ International Conference on Intelligent Robots and Systems*, 2015, pp. 2072–2078. 1
- [9] O. Salzman and D. Halperin, "Asymptotically-optimal motion planning using lower bounds on cost," in *IEEE International Conference on Robotics and Automation (ICRA)*, 2015, pp. 4167–4172. 1
- [10] J. D. Gammell, S. S. Srinivasa, and T. D. Barfoot, "Batch informed trees (BIT*): Sampling-based optimal planning via the heuristically guided search of implicit random geometric graphs," in *IEEE International Conference on Robotics and Automation (ICRA)*, 2015, pp. 3067–3074. 1
- [11] K. Solovey and D. Halperin, "Sampling-based bottleneck pathfinding with applications to Fréchet matching," in *European Symposium on Algorithms*, 2016, pp. 76:1–76:16. 1
- [12] L. E. Kavraki, M. N. Kolountzakis, and J. Latombe, "Analysis of probabilistic roadmaps for path planning," *IEEE Trans. Robotics and Automation*, vol. 14, no. 1, pp. 166–171, 1998. 1
- [13] A. M. Ladd and L. E. Kavraki, "Fast tree-based exploration of state space for robots with dynamics," in *Algorithmic Foundations of Robotics*, 2004, pp. 297–312. 1
- [14] S. Chaudhuri and V. Koltun, "Smoothed analysis of probabilistic roadmaps," *Comput. Geom.*, vol. 42, no. 8, pp. 731–747, 2009. 1
- [15] S. Karaman and E. Frazzoli, "Sampling-based algorithms for optimal motion planning," *International Journal of Robotics Research*, vol. 30, no. 7, pp. 846–894, 2011. 1, 3
- [16] N. H. Mustafa and K. Varadarajan, "Epsilon-nets and epsilon-approximations," in *Handbook of Discrete and Computational Geometry*, 3rd ed., J. E. Goodman, J. O'Rourke, and C. D. Toth, Eds. CRC Press LLC, 2016, ch. 47. [Online]. Available: <http://www.csun.edu/~ctoth/Handbook/HDCG3.html> 1
- [17] L. Janson, B. Ichter, and M. Pavone, "Deterministic sampling-based motion planning: Optimality, complexity, and performance," *International Journal of Robotics Research*, 2017. 1, 2, 3
- [18] A. Dobson and K. E. Bekris, "A study on the finite-time near-optimality properties of sampling-based motion planners," in *2013 IEEE/RSJ International Conference on Intelligent Robots and Systems, Tokyo, Japan, November 3-7, 2013*, 2013, pp. 1236–1241. 2
- [19] A. Dobson, G. V. Moustakides, and K. E. Bekris, "Geometric probability results for bounding path quality in sampling-based roadmaps after finite computation," in *IEEE International Conference on Robotics and Automation*, 2015, pp. 4180–4186. 2
- [20] K. Solovey, O. Salzman, and D. Halperin, "New perspective on sampling-based motion planning via random geometric graphs," *I. J. Robotics Res.*, vol. 37, no. 10, 2018. 2
- [21] K. Solovey and M. Kleinbort, "The critical radius in sampling-based motion planning," *The International Journal of Robotics Research*, 2019. 2
- [22] E. Schmerling, L. Janson, and M. Pavone, "Optimal sampling-based motion planning under differential constraints: The drift case with linear affine dynamics," in *IEEE Conference on Decision and Control*, 2015, pp. 2574–2581. 2
- [23] —, "Optimal sampling-based motion planning under differential constraints: The driftless case," in *IEEE International Conference on Robotics and Automation*, 2015, pp. 2368–2375. 2
- [24] B. Ichter, J. Harrison, and M. Pavone, "Learning sampling distributions for robot motion planning," in *Proc. IEEE Conf. on Robotics and Automation*, Brisbane, Australia, May 2018. [Online]. Available: <https://arxiv.org/pdf/1709.05448.pdf> 2
- [25] S. Choudhury, M. Bhardwaj, S. Arora, A. Kapoor, G. Ranade, S. Scherer, and D. Dey, "Data-driven planning via imitation learning," *I. J. Robotics Res.*, vol. 37, no. 13-14, 2018. [Online]. Available: <https://doi.org/10.1177/0278364918781001> 2
- [26] S. M. LaValle, *Planning Algorithms*. Cambridge, U.K.: Cambridge University Press, 2006. 2
- [27] J. Basch, L. J. Guibas, D. Hsu, and An Thai Nguyen, "Disconnection proofs for motion planning," in *IEEE International Conference on Robotics and Automation*, vol. 2, 2001, pp. 1765–1772. 3
- [28] Z. McCarthy, T. Bretl, and S. Hutchinson, "Proving path non-existence using sampling and alpha shapes," in *IEEE International Conference on Robotics and Automation*, 2012, pp. 2563–2569. 3
- [29] W. Reid, R. Fitch, A. Gktoan, and S. Sukkarieh, "Motion planning for reconfigurable mobile robots using hierarchical fast marching trees," in *Workshop on the Algorithmic Foundations of Robotics*, 2016. 4
- [30] B. Ichter and M. Pavone, "Robot motion planning in learned latent spaces," *IEEE Robotics and Automation Letters*, vol. 4, no. 3, pp. 2407–2414, 2019. 4

VIII. PROOFS

A. Proof of Theorem 1

We first present a simple version of the proof in Section VIII-A1 to help build intuition. Section VIII-A2 presents the proof of the necessary sample size result, which is similar in style to Section VIII-A1 with some more involved technical details. The proof of the necessary connection radius result is given in Section VIII-A3.

1) *Developing lower bounds:* Let $\{x_i\}_{i=1}^n$ be a sample set in $[0, 1]^d$. Suppose there is a ball of radius 2δ that does not intersect any of the points $\{x_i\}_{i=1}^n$. Let y denote the center of this ball. Consider the following environment:



The black dot is y . If the adversary chooses $x_{\text{start}} = y - \delta e_1$, $x_{\text{goal}} = y + \delta e_1$, denoted by the green and blue dots respectively, and obstacle set $\mathcal{F} := \{y\} \cup \{x : \|x - y\|_2 = 2\delta\}$ shown in black, then this problem is δ -clear, and a solution trajectory is shown in pink. Explicitly, a δ -clearance path for this environment is

$$p(t) := y - \delta \cos(\pi t)e_1 + \delta \sin(\pi t)e_2$$

which traces out a semicircle as t ranges in $[0, 1]$. There is, however, no way to reach x_{start} from x_{goal} in $G_{\mathcal{M}}$. This is because the obstacle $\{y\}$ blocks the edge between the start and the goal, and the shell $\{x : \|x - y\|_2 = 2\delta\}$ blocks any edges from these points to all points $\{x_i\}_{i=1}^n$. Thus, the nodes $x_{\text{start}}, x_{\text{goal}}$ will have no neighbors in $G_{\mathcal{M}}$.

Next, note that $y \in [2\delta, 1 - 2\delta]^d$ guarantees that $B_2(y, 2\delta) \subset [0, 1]^d$. Thus by Theorem 3, if $n < \sqrt{\pi d} (\sqrt{\frac{d}{2\pi e}} \frac{1-4\delta}{2\delta})^d$, then $\{x_i\}_{i=1}^n$ cannot be a 2δ -net of $[2\delta, 1 - 2\delta]^d$, which means there is a point $y \in [2\delta, 1 - 2\delta]^d$ at distance at least 2δ to all points in $\{x_i\}_{i=1}^n$. Thus, $B_2(y, 2\delta) \subset [0, 1]^d$ does not contain any points in $\{x_i\}_{i=1}^n$. Invoking the above argument for this y shows that $\{x_i\}_{i=1}^n$ will fail for the aforementioned obstacle scenario.

Thus, no deterministic planner using $n < \sqrt{\pi d} (\sqrt{\frac{d}{2\pi e}} \frac{1-4\delta}{2\delta})^d$ samples can be δ -complete in $[0, 1]^d$.

We first prove the necessary condition on n in Section VIII-A2, and then the necessary condition on r in Section VIII-A3.

2) *Necessary sample size:* Section VIII-A1 proves a weaker version of Theorem 1 by arguing that $(\mathcal{X}, r) \in \text{RM}(\delta)$ only if every ball of radius 2δ contains at least one point of \mathcal{X} . The proof technique we present here is similar, however, we will be working with rings instead of balls. The resulting necessary condition will be that every ring contained in $[0, 1]^d$ must contain at least one point of \mathcal{X} . This will lead to a stronger lower bound since the ring we will use is a subset of $B_2(0, 2\delta)$, giving rise to a more stringent necessary condition on \mathcal{X} than what was presented in Section VIII-A1.

To this end, we first define the following functions $y_\delta, y_\delta^\perp : [0, 2\pi] \rightarrow \mathbb{R}^d$ entry-wise:

$$(y_\delta(\theta))_i = \begin{cases} \delta \cos(\theta) & \text{if } i = 1 \\ \delta \sin(\theta) & \text{if } i = 2 \\ 0 & \text{else.} \end{cases} \quad \text{and} \quad (y_\delta^\perp(\theta))_i := \begin{cases} -\delta \sin(\theta) & \text{if } i = 1 \\ \delta \cos(\theta) & \text{if } i = 2 \\ 0 & \text{else.} \end{cases}$$

The vectors $\{y_\delta(\theta)\}_{\theta \in [0, 2\pi]}$ form a circle of radius δ centered at the origin in the subspace spanned by $\{e_1, e_2\}$, and $y_\delta^\perp(\theta) := \frac{d}{d\theta}y_\delta(\theta)$. Using this definition, we define the ring $\mathcal{R}(x_0, \delta, \delta)$ and the torus $\mathcal{T}(x_0, \delta, \delta)$ as

$$\begin{aligned}\mathcal{R}(x_0, \delta, \delta) &:= \{x_0 + y_\delta(\theta) + z : \theta \in [0, 2\pi], \|z\|_2 \leq \delta\} \\ \mathcal{T}(x_0, \delta, \delta) &:= \{x_0 + y_\delta(\theta) + z : \theta \in [0, 2\pi], \langle y_\delta^\perp(\theta), z \rangle = 0, \|z\|_2 = \delta\}.\end{aligned}$$

The volume of $\mathcal{R}(x_0, \delta, \delta)$ is $(2\pi\delta)(c_{d-1}\delta^{d-1}) = 2\pi c_{d-1}\delta^d$. $\mathcal{T}(x_0, \delta, \delta)$ is the boundary of $\mathcal{R}(x_0, \delta, \delta)$. Our goal is to cover the set \mathcal{D} with rings where

$$\mathcal{D} := [2\delta, 1 - 2\delta] \times [2\delta, 1 - 2\delta] \times [\delta, 1 - \delta]^{d-2}.$$

We choose to cover \mathcal{D} because $x_0 \in \mathcal{D}$ is an equivalent condition for $\mathcal{R}(x_0, \delta, \delta) \subset [0, 1]^d$. If a set of points $\{x_i\}_{i=1}^n$ satisfies $\mathcal{D} \subset \bigcup_{i=1}^n \mathcal{R}(x_i, \delta, \delta)$, then

$$\begin{aligned}\text{vol}(\mathcal{D}) &\leq \text{vol}\left(\bigcup_{i=1}^n \mathcal{R}(x_i, \delta, \delta)\right) \\ \implies (1 - 4\delta)^2 (1 - 2\delta)^{d-2} &\leq \text{vol}\left(\bigcup_{i=1}^n \mathcal{R}(x_i, \delta, \delta)\right) \\ &\leq n 2\pi c_{d-1} \delta^d \\ \text{See Section IX-D} \rightarrow &= n 2\pi \sqrt{\frac{1}{\pi(d-1)}} \left(\sqrt{\frac{2\pi e}{d-1}}\right)^{d-1} \delta^d \\ \implies n &\geq \sqrt{\frac{2\pi e}{d-1}} \frac{\sqrt{\pi(d-1)}}{2\pi} \left(1 - \frac{2\delta}{1-2\delta}\right)^2 \left(\sqrt{\frac{d-1}{2\pi e}} \frac{(1-2\delta)}{\delta}\right)^d \\ &= \sqrt{\frac{e}{2}} \left(1 - \frac{2\delta}{1-2\delta}\right)^2 \left(\sqrt{\frac{d-1}{2\pi e}} \frac{(1-2\delta)}{\delta}\right)^d\end{aligned}$$

Therefore, if $n < \sqrt{\frac{e}{2}} \left(1 - \frac{2\delta}{1-2\delta}\right)^2 \left(\sqrt{\frac{d-1}{2\pi e}} \frac{(1-2\delta)}{\delta}\right)^d$, then for any collection of points $\{x_i\}_{i=1}^n$, there is a point $x^* \in \mathcal{D}$ so that $x^* \notin \mathcal{R}(x_i, \delta, \delta)$ for every $1 \leq i \leq n$. This means that $x_i \notin \mathcal{R}(x^*, \delta, \delta)$ for every i . We can show this by contradiction. Suppose $x_i \in \mathcal{R}(x^*, \delta, \delta)$. Then we can write $x_i = x^* + y_\delta(\theta) + z$ for some $\theta \in [0, 2\pi]$ and $\|z\|_2 \leq \delta$. But then choosing $\theta' = \theta + \pi \pmod{2\pi}$ and $z' = -z$ gives $y_\delta(\theta') = -y_\delta(\theta)$ and we can then write $x^* = x_i + y' + z'$, meaning $x^* \in \mathcal{R}(x_i, \delta, \delta)$ which is a contradiction.

Given this point x^* , consider the motion-planning problem

$$\begin{aligned}\overline{\mathcal{F}} &= \mathcal{T}(x^*, \delta, \delta) \\ x_{\text{start}} &= x^* + \delta e_1 \\ x_{\text{goal}} &= x^* - \delta e_1.\end{aligned}$$

The path

$$p(t) := x^* + y_\delta(\pi t), t \in [0, 1]$$

is a feasible δ -clearance path, because by definition, $\mathcal{R}(x^*, \delta, \delta)$ is the set of points within δ of p , and obstacles only exist at $\mathcal{T}(x^*, \delta, \delta)$, which is the boundary of $\mathcal{T}(x^*, \delta, \delta)$. This means all points in the obstacle set are at distance at least δ from all points in p . Note that constructing a graph G based on collision free line segments between $\{x_i\}_{i=1}^n \cup \{x_{\text{start}}, x_{\text{goal}}\}$ will not have a path from x_{start} to x_{goal} . This is because $x^* \notin \mathcal{F}$, (indeed, set $\theta = 0, z = -\delta e_1$), therefore there cannot be an edge directly from x_{start} to x_{goal} . Thus, a path from x_{start} to x_{goal} must include at least one point from $\{x_i\}_{i=1}^n$. However, by construction, all points in $\{x_i\}_{i=1}^n$ are in $\overline{\mathcal{R}}(x^*, \delta, \delta)$, while $x_{\text{start}}, x_{\text{goal}} \in \mathcal{R}(x^*, \delta, \delta)$. Thus any line segment joining a point in $\{x_i\}_{i=1}^n$ to $\{x_{\text{start}}, x_{\text{goal}}\}$ must pass through the boundary of the ring, $\mathcal{T}(x^*, \delta, \delta)$, which is an obstacle. Therefore the nodes $x_{\text{start}}, x_{\text{goal}}$ are isolated in G , i.e. they have no neighbors. Thus there is no path from the start to the goal in G for this obstacle environment.

3) *Necessary connection radius:* From Theorem 3, we know that any ϵ -net of $[\delta, 1 - \delta]^d$ must have at least $\sqrt{\pi d} \left(\sqrt{\frac{d}{2\pi e} \frac{1-2\delta}{\epsilon}} \right)^d$ points. Therefore, if $n < \sqrt{\pi d} \left(\sqrt{\frac{d}{2\pi e} \frac{1-2\delta}{\epsilon}} \right)^d$, then there exists no set of n points which is an ϵ -net. Note that

$$\begin{aligned} n &< \sqrt{\pi d} \left(\sqrt{\frac{d}{2\pi e} \frac{1-2\delta}{\epsilon}} \right)^d \\ \iff \left(\frac{n}{\sqrt{\pi d}} \right)^{1/d} &< \sqrt{\frac{d}{2\pi e} \frac{1-2\delta}{\epsilon}} \\ \iff \epsilon &< (1-2\delta) \sqrt{\frac{d}{2\pi e}} \left(\frac{\sqrt{\pi d}}{n} \right)^{1/d}. \end{aligned}$$

Now for any $r < (1-2\delta) \sqrt{\frac{d}{2\pi e}} \left(\frac{\sqrt{\pi d}}{n} \right)^{1/d}$, there cannot exist a r -net of size n . Therefore, for any $\{x_i\}_{i=1}^n$, there exists $x^* \in [\delta, 1 - \delta]^d$ so that $\|x_i - x^*\|_2 > r$ for every $i \in [n]$. If we choose $x_{\text{start}} = x^*$ and x_{goal} satisfying $\|x_{\text{start}} - x_{\text{goal}}\|_2 > r$, then the PRM graph induced by the connection radius r and vertices $\{x_i\}_{i=1}^n \cup \{x_{\text{start}}, x_{\text{goal}}\}$ will have no edges connecting to x_{start} , since there are no points within r of x_{start} . As a consequence, the induced graph will not have a path from x_{start} to x_{goal} .

B. Proof of Theorem 2

1) *Proof Intuition:* Suppose \mathcal{M} is a δ_{\min} -clearance motion planning problem. It then has a shortest δ_{\min} -clear solution p . Consider points $\{p_j\}_{j=1}^m$ on the path p so that consecutive points are at $2\sqrt{1-\alpha^2}\delta_{\min}$ euclidean distance apart. See Fig. 3 for an illustration. For each $1 \leq j \leq m-1$, by δ_{\min} -clearance the balls of radius δ_{\min} centered at p_j, p_{j+1} are collision free. This is illustrated by the blue region in Fig. 3. If we have a collection of samples \mathcal{X} which forms a $\alpha\delta_{\min}$ -net of the space, then we are guaranteed that there are $z_j, z_{j+1} \in \mathcal{X}$ that are within $\alpha\delta$ distance of p_j and p_{j+1} respectively. This is illustrated by the green regions. The condition on n given in the statement of Theorem 2 guarantees the existence of such a \mathcal{X} . The spacing $2\sqrt{1-\alpha^2}\delta_{\min}$ was chosen so that the convex hull of the green set, depicted as the union of the green and violet regions, is entirely contained in the blue, collision free region. This means that any line segment joining a point in the left green ball to a point in the right green ball is entirely contained in the blue region, hence it is collision-free. Therefore, for each j , the line segment joining z_j to z_{j+1} is collision-free for every $1 \leq j \leq m-1$. Furthermore, by triangle inequality, the length of these segments can be at most $2(\alpha + \sqrt{1-\alpha^2})\delta_{\min}$. Thus, if we choose r to be this value, then the edges $\{(z_j, z_{j+1})\}_{j=1}^{m-1}$ will all be in the graph $G_{\mathcal{M}}(\mathcal{X}, r)$. Since p is a solution path, we can choose the first and last samples $p_1 = x_{\text{start}}$ and $p_m = x_{\text{goal}}$. Therefore the path that concatenates these edges will be a collision-free path from the start to the goal in the graph $G_{\mathcal{M}}(\mathcal{X}, r)$. Finally, to bound the length of this path, note that the length of the path from p_j to p_{j+1} is at least $\|p_j - p_{j+1}\|_2 = 2\sqrt{1-\alpha^2}\delta_{\min}$. We then have

$$\frac{\|z_j - z_{j+1}\|_2}{\|p_j - p_{j+1}\|_2} \leq \frac{2(\alpha + \sqrt{1-\alpha^2})\delta_{\min}}{2\sqrt{1-\alpha^2}\delta_{\min}} = 1 + \frac{\alpha}{\sqrt{1-\alpha^2}} = 1 + \epsilon$$

where the last equality is due to the definition of α . Since each piece of the path defined by $\{z_j\}_{j=1}^m$ is not more than $1 + \epsilon$ times its corresponding piece in p , this gives a path whose total length is at most $1 + \epsilon$ times the length of p . In the remainder of this section we formalize this intuition into a proof of Theorem 2.

2) *Proof setup:* We now formally construct a proof based on the intuition of the previous section. Fix $\epsilon, \delta \in (0, 1)$ and a δ -clear motion planning problem \mathcal{M} . Define $\alpha := \frac{\epsilon}{\sqrt{1+\epsilon^2}}$. Suppose we have n satisfying

$$n \geq \sqrt{\pi d} \left(\sqrt{\frac{2d}{\pi e} \frac{1-(2-\alpha)\delta}{\alpha\delta}} \right)^d.$$

Define δ_{\min} so that

$$n = \sqrt{\pi d} \left(\sqrt{\frac{2d}{\pi e} \frac{1-(2-\alpha)\delta_{\min}}{\alpha\delta_{\min}}} \right)^d. \quad (1)$$

Two immediate consequences of this definition are that $\delta_{\min} \leq \delta$ and

$$\begin{aligned} \delta_{\min} &= \frac{1-(2-\alpha)\delta_{\min}}{\alpha} \sqrt{\frac{2d}{\pi e}} \left(\frac{\sqrt{\pi d}}{n} \right)^{1/d} \\ \implies \delta_{\min} &< \frac{1}{\alpha} \sqrt{\frac{2d}{\pi e}} \left(\frac{\sqrt{\pi d}}{n} \right)^{1/d}. \end{aligned} \quad (2)$$

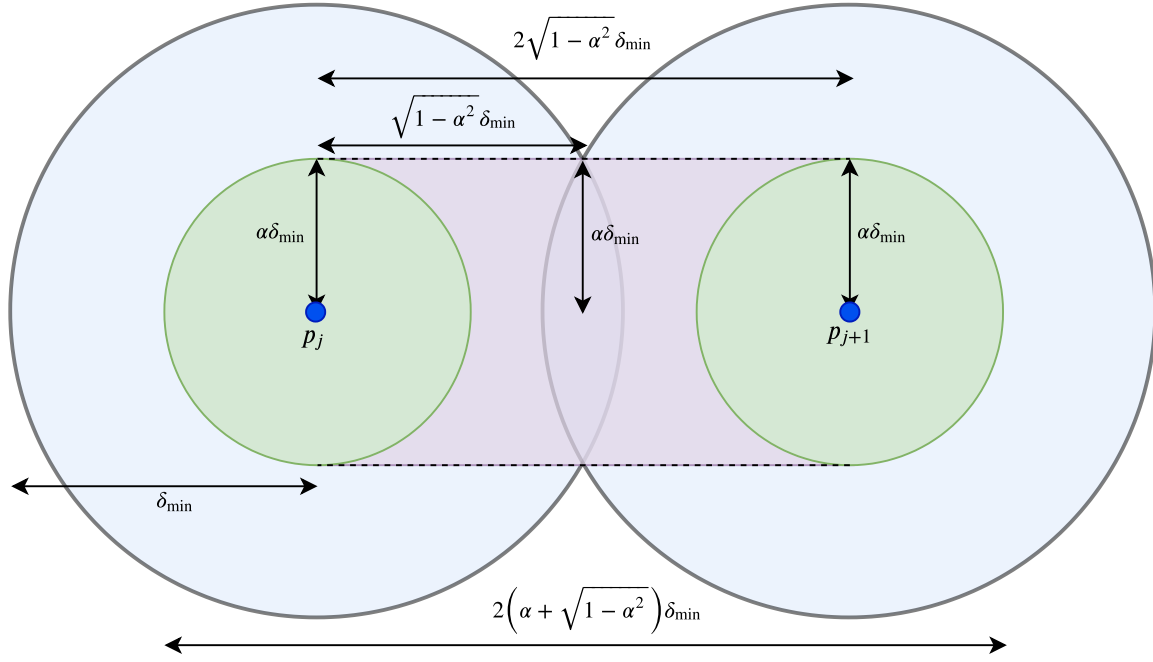


Figure 3. A visualization of the proof technique of Theorem 2 in 2 dimensions.

Let $p : [0, 1] \rightarrow [0, 1]^d$ be the shortest¹ δ -clear path for \mathcal{M} . Choose $\{t_j\}_{j=1}^m$ so that:

- 1) $t_1 = 0$ and $t_m = 1$.
- 2) $t_j < t_k$ whenever $j < k$.
- 3) $\|p_j - p_{j+1}\|_2 = 2\sqrt{1 - \alpha^2}\delta_{\min}$ for all $1 \leq j \leq m - 1$ where $p_j := p(t_j)$.

Since p has δ clearance, $p([0, 1]) \subset [\delta, 1 - \delta]^d$. Since $\delta_{\min} \leq \delta$ we have $[\delta, 1 - \delta]^d \subset [\delta_{\min}, 1 - \delta_{\min}]^d$. Note that $[\delta_{\min}, 1 - \delta_{\min}]^d \oplus B_2(0, \frac{\alpha\delta_{\min}}{2})$ is contained in a hypercube of side length $1 - (2 - \alpha)\delta_{\min}$. Thus by Theorem 3, the condition in (1) ensures that we can choose $\{x_i\}_{i=1}^n$ to be an $\alpha\delta_{\min}$ -net of $[\delta_{\min}, 1 - \delta_{\min}]^d$. In particular, for every j , there exists $z_j \in \{x_i\}_{i=1}^n$ so that $\|p_j - z_j\|_2 \leq \alpha\delta_{\min}$.

To prove the existence of a path from x_{start} to x_{goal} we will show the following two statements are true:

- 1) The line segments connecting z_j to z_{j+1} are collision free for all $1 \leq j \leq m - 1$.
- 2) $\|z_j - z_{j+1}\|_2 \leq 2(\alpha + \sqrt{1 - \alpha^2})\delta_{\min}$.

Once we establish these statements, we will choose a connection radius r larger than $2(\alpha + \sqrt{1 - \alpha^2})\delta_{\min}$. This ensures that the edges $\{(z_j, z_{j+1})\}_{j=1}^{m-1}$ will all be in the resulting graph $G_{\mathcal{M}}(\{x_i\}_{i=1}^n, r)$. The path we construct will then be a concatenate all of the (z_j, z_{j+1}) collision-free edges to get a collision-free path from the start to the goal.

3) *Proving $\text{co}(\{z_j, z_{j+1}\})$ is collision-free:* This is equivalent to saying that $\beta z_j + (1 - \beta)z_{j+1} \in \mathcal{F}$ for every $\beta \in [0, 1]$. Since p_j, p_{j+1} are points on a δ -clear path, the balls $B_2(p_j, \delta), B_2(p_{j+1}, \delta)$ are collision-free. Thus it suffices to show $\text{co}(\{z_j, z_{j+1}\}) \subset B_2(p_j, \delta_{\min}) \cup B_2(p_{j+1}, \delta_{\min})$ for each j . For any $\beta \in [0, 1]$, let $u_\beta := \beta z_j + (1 - \beta)z_{j+1}$, and

$$v_\beta := \underset{v \in \text{co}(\{p_i, p_{i+1}\})}{\text{argmin}} \|u_\beta - v\|_2.$$

By triangle inequality we have

$$\|\beta z_j + (1 - \beta)z_{j+1} - \beta p_j + (1 - \beta)p_{j+1}\|_2 \leq \beta \|z_j - p_j\|_2 + (1 - \beta) \|z_{j+1} - p_{j+1}\|_2 \leq \alpha\delta_{\min},$$

and thus $\|u_\beta - v_\beta\|_2 \leq \alpha\delta_{\min}$. If $v_\beta = p_j$, then $\|u_\beta - p_j\|_2 \leq \alpha\delta_{\min}$ implies that $u_\beta \in B_2(p_j, \delta_{\min})$, since $\alpha \leq 1$. Similarly, if $v_\beta = p_{j+1}$ then $u_\beta \in B_2(p_{j+1}, \delta_{\min})$. If v_β is not one of the endpoints, we can write $v_\beta = \beta^* p_j + (1 - \beta^*) p_{j+1}$ where

$$\beta^* = \arg \min_{\beta \in (0, 1)} \|u_\beta - \beta p_j + (1 - \beta)p_{j+1}\|_2^2.$$

¹Technically we need to say ‘‘arbitrarily close to the infimum length of a δ -clear path’’ here.

As a consequence of the first order optimality conditions, we have $\langle p_{j+1} - p_j, u_\beta - v_\beta \rangle = 0$. Since the points $\{p_j, p_{j+1}, v_\beta\}$ are collinear, we also have

$$\langle v_\beta - p_j, u_\beta - v_\beta \rangle = \langle v_\beta - p_{j+1}, u_\beta - v_\beta \rangle = 0.$$

There are now two cases. If $\beta^* \leq 1/2$, we have

$$\begin{aligned} \|u_\beta - p_{j+1}\|_2^2 &= \|(u_\beta - v_\beta) + (v_\beta - p_{j+1})\|_2^2 \\ &= \|u_\beta - v_\beta\|_2^2 + \|v_\beta - p_{j+1}\|_2^2 \\ &\leq \alpha^2 \delta_{\min}^2 + \|\beta^* p_j + (1 - \beta^*) p_{j+1} - p_{j+1}\|_2^2 \\ &= \alpha^2 \delta_{\min}^2 + (\beta^*)^2 \|p_j - p_{j+1}\|_2^2 \\ &= \alpha^2 \delta_{\min}^2 + (\beta^*)^2 4(1 - \alpha^2) \delta_{\min}^2 \\ &\leq \delta_{\min}^2. \end{aligned}$$

Otherwise, we have $\beta^* > 1/2$, where we see that

$$\begin{aligned} \|u_\beta - p_j\|_2^2 &= \|(u_\beta - v_\beta) + (v_\beta - p_j)\|_2^2 \\ &= \|u_\beta - v_\beta\|_2^2 + \|v_\beta - p_j\|_2^2 \\ &\leq \alpha^2 \delta_{\min}^2 + \|\beta^* p_j + (1 - \beta^*) p_{j+1} - p_j\|_2^2 \\ &= \alpha^2 \delta_{\min}^2 + (1 - \beta^*)^2 \|p_j - p_{j+1}\|_2^2 \\ &= \alpha^2 \delta_{\min}^2 + (1 - \beta^*)^2 4(1 - \alpha^2) \delta_{\min}^2 \\ &\leq \delta_{\min}^2. \end{aligned}$$

In either case, $u_\beta \in B_2(p_j, \delta_{\min}) \cup B_2(p_{j+1}, \delta_{\min}) \subset B_2(p_j, \delta) \cup B_2(p_{j+1}, \delta)$. Since this is true for every $\beta \in [0, 1]$, the edge joining z_j to z_{j+1} is collision-free.

4) *Proving z_j, z_{j+1} are close together:* Furthermore, by triangle inequality we have

$$\begin{aligned} \|z_j - z_{j+1}\|_2 &= \|(z_j - p_j) + (p_j - p_{j+1}) + (p_{j+1} - z_{j+1})\|_2 \\ &\leq \|z_j - p_j\|_2 + \|p_j - p_{j+1}\|_2 + \|p_{j+1} - z_{j+1}\|_2 \\ &= \alpha \delta_{\min} + 2\sqrt{1 - \alpha^2} \delta_{\min} + \alpha \delta_{\min} \\ &= 2\left(\alpha + \sqrt{1 - \alpha^2}\right) \delta_{\min} \\ &\stackrel{(a)}{<} \frac{2}{\alpha} \left(\alpha + \sqrt{1 - \alpha^2}\right) \sqrt{\frac{2d}{\pi e}} \left(\frac{\sqrt{\pi d}}{n}\right)^{1/d} \\ &\stackrel{(b)}{=} 2\left(1 + \frac{1}{\epsilon}\right) \sqrt{\frac{2d}{\pi e}} \left(\frac{\sqrt{\pi d}}{n}\right)^{1/d}. \end{aligned}$$

Where (a) is due to (2) and (b) is due to the definition of α . Thus setting $r = 2\left(1 + \frac{1}{\epsilon}\right) \sqrt{\frac{2d}{\pi e}} \left(\frac{\sqrt{\pi d}}{n}\right)^{1/d}$, then the edges $\{(z_j, z_{j+1})\}_{j=1}^{m-1}$ will all be present in the PRM graph. Concatenating these segments gives a feasible path from x_{start} to x_{goal} .

5) *Establishing $(1 + \epsilon)$ -optimality:* Finally we bound the length of the path. Denote by $\ell(p)$ the length of p , and let z be the path induced by the concatenation of the straight lines connecting z_1, z_2, \dots, z_{m-1} , respectively.

$$\begin{aligned} \ell(z) &= \sum_{j=1}^{m-1} \|z_{j+1} - z_j\|_2 \leq \sum_{j=1}^{m-1} \|z_{j+1} - p_{j+1}\|_2 + \|p_{j+1} - p_j\|_2 + \|z_j - p_j\|_2 \\ &= \sum_{j=1}^{m-1} \|p_{j+1} - p_j\|_2 \left(\frac{\|z_{j+1} - p_{j+1}\|_2 + \|p_{j+1} - p_j\|_2 + \|z_j - p_j\|_2}{\|p_{j+1} - p_j\|_2} \right) \\ &\leq \sum_{j=1}^{m-1} \|p_{j+1} - p_j\|_2 \left(1 + \frac{2\alpha \delta_{\min}}{2\sqrt{1 - \alpha^2} \delta_{\min}} \right) = \left(1 + \frac{\alpha}{\sqrt{1 - \alpha^2}} \right) \sum_{j=1}^{m-1} \|p_{j+1} - p_j\|_2 \\ &\leq \left(1 + \frac{\alpha}{\sqrt{1 - \alpha^2}} \right) \ell(p) \stackrel{(a)}{=} (1 + \epsilon) \ell(p). \end{aligned}$$

where (a) is due to the definition of α , which implies that $\frac{\alpha}{\sqrt{1 - \alpha^2}} = \epsilon$.

IX. APPENDIX FOR AUXILIARY RESULTS

A. Proof of Theorem 3

Suppose \mathcal{Y} is an ϵ -net of \mathcal{X} . To show the first part, note that

$$\begin{aligned} \mathcal{X} &\subset \bigcup_{y \in \mathcal{Y}} B_2(y, \epsilon) \\ \implies \text{vol}(\mathcal{X}) &\leq \text{vol}\left(\bigcup_{y \in \mathcal{Y}} B_2(y, \epsilon)\right) \\ &\leq \sum_{y \in \mathcal{Y}} \text{vol}(B_2(y, \epsilon)) \\ &= |\mathcal{Y}| c_d \epsilon^d, \end{aligned}$$

and thus $|\mathcal{Y}| \geq \frac{\text{vol}(\mathcal{X})}{c_d \epsilon^d}$.

To conclude, we note that c_d is a function of d , where the dependence is described in Section IX-D. Substituting the expression obtained in Section IX-D into these bounds we obtain

$$|\mathcal{Y}| \geq \text{vol}(\mathcal{X}) \sqrt{\pi d} \left(\sqrt{\frac{d}{2\pi e}}\right)^d \frac{1}{\epsilon^d} = \text{vol}(\mathcal{X}) \sqrt{\pi d} \left(\sqrt{\frac{d}{2\pi e}} \frac{1}{\epsilon}\right)^d.$$

For the second part, we construct an ϵ -net via Algorithm 1.

For \mathcal{Y} the output of such a procedure, note that by construction, all distinct members of \mathcal{Y} are at distance at least ϵ . Therefore, if $y_1, y_2 \in \mathcal{Y}$ with $y_1 \neq y_2$, we have $B_2(y_1, \epsilon/2) \cap B_2(y_2, \epsilon/2) = \emptyset$. Also note that $y \in \mathcal{X}$ implies that $B_2(y, \epsilon/2) \in \mathcal{X} \oplus B_2(0, \epsilon/2)$. Therefore, we have

$$\begin{aligned} \mathcal{X} \oplus B_2\left(y, \frac{\epsilon}{2}\right) &\supset \bigcup_{y \in \mathcal{Y}} B_2\left(y, \frac{\epsilon}{2}\right) \\ \implies \text{vol}\left(\mathcal{X} \oplus B_2\left(y, \frac{\epsilon}{2}\right)\right) &\geq \text{vol}\left(\bigcup_{y \in \mathcal{Y}} B_2\left(y, \frac{\epsilon}{2}\right)\right) \\ &= \sum_{y \in \mathcal{Y}} \text{vol}\left(B_2\left(y, \frac{\epsilon}{2}\right)\right) \\ &= |\mathcal{Y}| c_d \left(\frac{\epsilon}{2}\right)^d, \end{aligned}$$

therefore $|\mathcal{Y}| \leq \frac{1}{c_d} \left(\frac{2}{\epsilon}\right)^d \text{vol}\left(\mathcal{X} \oplus B_2\left(y, \frac{\epsilon}{2}\right)\right)$. Substituting the dependence of c_d on d (See Section IX-D we obtain

$$|\mathcal{Y}| \leq \text{vol}\left(\mathcal{X} \oplus B_2\left(y, \frac{\epsilon}{2}\right)\right) \sqrt{\pi d} \left(\sqrt{\frac{2d}{\pi e}} \frac{1}{\epsilon}\right)^d.$$

B. Proof of Lemma 1

We have $|\mathcal{X}_{\text{grid}}(w)| = \left(\frac{1}{w}\right)^d$, we have

$$[0, 1]^d = \bigsqcup_{x \in \mathcal{X}_{\text{grid}}(w)} B_\infty\left(x, \frac{w}{2}\right),$$

therefore $\max_{y \in [0, 1]^d} d(y, \mathcal{X}_{\text{grid}}(w)) = \frac{\sqrt{dw}}{2}$. So if we want $\mathcal{X}_{\text{grid}}(w)$ a ϵ -net, then we need $w = \frac{2\epsilon}{\sqrt{d}}$. This gives $\left|\mathcal{X}_{\text{grid}}\left(\frac{2\epsilon}{\sqrt{d}}\right)\right| = \left(\frac{\sqrt{d}}{2\epsilon}\right)^d$. The proof of Theorem 3 gives a construction of a ϵ -net \mathcal{X} of $[0, 1]^d$ whose size is $|\mathcal{X}| \leq \text{vol}\left([0, 1]^d \oplus B_2\left(0, \frac{\epsilon}{2}\right)\right) \sqrt{\pi d} \left(\sqrt{\frac{2d}{\pi e}} \frac{1}{\epsilon}\right)^d$. Comparing these two ϵ -nets we see

$$\begin{aligned}
\frac{|\mathcal{X}|}{\left| \mathcal{X}_{\text{grid}} \left(\frac{2\epsilon}{\sqrt{d}} \right) \right|} &< (1 + \epsilon)^d \frac{\sqrt{\pi d} \left(\sqrt{\frac{2d}{\pi e}} \frac{1}{\epsilon} \right)^d}{\left(\frac{\sqrt{d}}{2\epsilon} \right)^d} \\
&= \sqrt{\pi d} \left((1 + \epsilon) \sqrt{\frac{2d}{\pi e}} \frac{1}{\epsilon} \frac{2\epsilon}{\sqrt{d}} \right)^d \\
&= \sqrt{\pi d} \left(\frac{\sqrt{8}(1 + \epsilon)}{\sqrt{\pi e}} \right)^d
\end{aligned}$$

When $\epsilon < \sqrt{\frac{\pi e}{8}} - 1$ we have $\frac{\sqrt{8}(1+\epsilon)}{\sqrt{\pi e}} < 1$, hence the ratio goes to zero as $d \rightarrow \infty$. We can then conclude that there exist ϵ -nets that are more efficient than grids for high dimensional problems.

C. Proof for Corollary 1

Throughout this proof we let $\alpha := \frac{\epsilon}{\sqrt{1+\epsilon^2}}$. In the proof of Theorem 2 from Section VIII-B, we showed that if \mathcal{X} is a $\alpha\delta$ -net and $r \geq 2(\alpha + \sqrt{1-\alpha^2})\delta$, then $(\mathcal{X}, r) \in \text{RM}(\delta)$ with δ -stretch at most $1 + \epsilon$. Due to norm equivalence, to obtain a $\alpha\delta$ net using a grid, the grid spacing w must be at most $\frac{2\alpha\delta}{\sqrt{d}}$. Since the solution path p is δ -clear, it must be at distance at least δ from the boundary of $[0, 1]^d$, hence it is entirely contained in $[\delta, 1 - \delta]^d$. Thus to ensure δ -completeness with stretch at most $1 + \epsilon$, we need to construct a grid of $[\delta, 1 - \delta]^d$ with spacing $\frac{2\alpha\delta}{\sqrt{d}}$. A grid of $[\delta, 1 - \delta]^d$ with spacing $\frac{2\alpha\delta}{\sqrt{d}}$ has exactly $\frac{\sqrt{d}(1-2\delta)}{2\alpha\delta}$ points along each axis, hence

$$\left| \mathcal{X}_{\text{grid}} \left(\frac{2\alpha\delta}{\sqrt{d}} \right) \right| = \left(\frac{\sqrt{d}(1-2\delta)}{2\alpha\delta} \right)^d.$$

D. Unit Ball Volume Approximation

We begin by defining the gamma function $\Gamma : \mathbb{R}_+ \rightarrow \mathbb{R}_+$ as

$$\Gamma(x) := \int_0^\infty t^{x-1} e^{-t} dt.$$

A simple consequence of integration by parts is that for positive integer n , $\Gamma(n) = (n-1)!$. For general real numbers, the gamma function has no closed form expression. We do have good approximations, described by the following result:

Theorem 4 (Stirling's Approximation).

$$\lim_{x \rightarrow \infty} \frac{\Gamma(x+1)}{\sqrt{2\pi x} \left(\frac{x}{e} \right)^x} = 1,$$

and we have the following bounds for finite x :

$$\sqrt{2\pi x} \left(\frac{x}{e} \right)^x \leq \Gamma(x+1) \leq e\sqrt{x} \left(\frac{x}{e} \right)^x.$$

It is known that the volume of the unit ball in d dimensions is

$$c_d := \frac{\pi^{d/2}}{\Gamma\left(\frac{d}{2} + 1\right)}.$$

we obtain the desired result by applying Stirling's approximation to bound c_d^{-1} .

$$c_d^{-1} = \frac{\Gamma\left(\frac{d}{2} + 1\right)}{\pi^{d/2}} \sim \sqrt{2\pi \frac{d}{2}} \left(\frac{d}{2e} \right)^{d/2} \frac{1}{\pi^{d/2}} = \sqrt{\pi d} \left(\sqrt{\frac{d}{2\pi e}} \right)^d.$$